Enhancing Compressive Strength and Dentin Interaction of Mineral Trioxide Aggregate by Adding SrO and Hydroxyapatite

Leny Yuliatun[1], Eko Sri Kunarti[1], Widjijono Widjijono[2], and Nuryono Nuryono[1*]

[1]*Department of Chemistry, Faculty of Mathematics and Natural Sciences, Universitas Gadjah Mada, Sekip Utara, Yogyakarta 55281, Indonesia*

[2]*Department of Dental Biomaterials, Faculty of Dentistry, Universitas Gadjah Mada, Jl. Denta 1, Sekip Utara, Yogyakarta 55281, Indonesia*

* ***Corresponding author:***

email: nuryono_mipa@ugm.ac.id

Received: July 13, 2022
Accepted: September 2, 2022

DOI: 10.22146/ijc.76231

Abstract: *In this research, the effect of strontium oxide (SrO) and hydroxyapatite (HA) on the properties of mineral trioxide aggregate (MTA) have been studied. MTA contained 20% SiO_2, 60% CaO, and 2% Al_2O_3. Bi_2O_3 and SrO have been added with 18% (w/w) total percentage. MTA was prepared with a sol-gel process using a weak base (NH_3) as a catalyst and calcined at 1000 °C for 3 h. The effect of HA was investigated by adding various percentages (3, 6, and 9%) on the MTA modified with 5% SrO. The modified MTA (MTA-SrO-HA) products were hydrated using water with the MTA to water weight ratio of 3:1. The results showed that tricalcium silicate (C_3S), dicalcium silicate (C_2S), Bi_2O_3, and strontium silicate peaks were detected in the XRD patterns. An increase in the intensity in the infrared spectra of CaO occurred after hybridization with HA. In addition, bonding of Ca-O-Si appeared at 879 and 995 cm^{-1}, indicating the formation of cement. MTA modified with 5% SrO and 6% HA showed similar compressive strength to the commercial MTA (ProRoot brand). Furthermore, MTA-SrO5/HA6 showed a strong interface interaction with dentin adheres without any gaps, indicating a potential dental material for the future.*

Keywords: *MTA; SrO; hydroxyapatite; strontium silicate*

■ INTRODUCTION

Various commercial brands of mineral trioxide aggregate (MTA) are sold to treat tooth roots, including ProRoot, MTA Angelus, Biodentine, Endocem MTA, DiaRoot, Retro MTA, Rootdent, Endocem Zr, and Bioaggregate. The MTA composition has 80% Portland cement and 20% bismuth trioxide to supply radiopacity properties [1]. MTA provides good biocompatibility and an effective dental covering because it has unique properties and advantages over other dental materials [2]. Therefore, it is commonly applied for clinical applications in teeth [3]. On the other hand, the disadvantages of MTA are the presence of bubbles during cementation, which causes gaps, cavities, and pores, indeterminate setting time and compressive strength, and relatively expensive. Increasing the compressive strength and dentin interaction with MTA can be done by adding SrO particles.

Proper and uniform MTA particle size can be controlled using an additive, such as bismuth oxide (Bi_2O_3) and strontium oxide (SrO). These particles lead to favorable density and can protect teeth roots well [4]. In addition, SrO is safe, non-toxic, analogous to calcium, and can increase the compressive strength of MTA material. SrO can also act as the provider of radiopacity in the material besides Bi_2O_3. Strontium oxide is used as a radiopacity agent in MTA to form strontium silicate, which is used as a component to increase radiopacity bioactivity for better tubular occlusion [5].

The existence of Sr ions can inhibit mineralized tissue, such as osteodentin, in mash tissue. Hence, strontium, in combination with other materials, can be utilized as a modern pulp-capping MTA [6]. The excellent biocompatibility of MTA can be obtained by adding about 5% strontium to prevent agglomeration

and uniform distribution of particles [7]. Sr^{2+} can substitute Ca^{2+} in the material when applied to produce a coupling with tricalcium phosphate in saliva [8].

Several efforts to improve the adhesion and biocompatibility of MTA with dentine have been reported widely by modifying it with other materials, such as hydroxyapatite (HA). The mixture can release calcium ions into the environment around the pulp with a high pH and allows hard-tissue regeneration [9]. HA also has a higher potential for odontogenic and differentiation properties than MTA. Thus, regenerative therapy can be designed for the dentin layer of teeth [10]. HA can be used as an internal matrix and furcation perforation material to reconstruct dental root tissue [11]. Additionally, HA has the highest bioactivity among other types of cement [12] to repair and glue damaged hard tissues [13].

The synthesized MTA has weaknesses in terms of compressive strength and dentin interaction. These characteristics can be improved by adding SrO and HA to become composite materials. Composite prepared from MTA composition combined with SrO and HA (MTA-SrO/HA) has not been reported. Therefore, this research aims to improve compressive strength characteristics and dentin interaction from synthesized MTA by adding SrO and HA. The properties of the composite also evaluated include weight loss, calcium ions release, and pH after hydration.

■ EXPERIMENTAL SECTION

Materials

Materials used for the synthesis of MTA-SrO and MTA-SrO/HA were bismuth trioxide (Bi_2O_3) (99% purity), $Al(NO_3)_3{\cdot}9H_2O$ (99%), and $CaCO_3$ (99%). Tetraethoxyorthosilicate (TEOS, 99% purity) was used as a silica source, and an ammonia solution (25%) was used as a catalyst. Other materials used for the modification were strontium carbonate ($SrCO_3$, 98%) and hydroxyapatite (HA, 99%). The materials used in this research were purchased from Sigma-Aldrich, Germany, and used without previous treatment.

Instrumentation

The types of equipment used to characterize materials included DTA/TGA (Toyo Kasegyo M-300 KS), X-Ray Fluorescence (RIGAKU–NEX QC+QuanTEZ), Expert Pro X-Ray Diffraction scanned at $2\theta = 5–80°$ and 8201PC Shimadzu Fourier Transform Infrared. Other types of equipment were JEOL Scanning Electron Microscopy, Analytic Jena Atomic Absorption Spectrophotometer, Mettler Toledo pH meter, and Dental X-ray. Texture Analyzer CT3 Merck Brookfield UTM was used for the compressive strength test.

Procedure

Synthesis of MTA-SrO and MTA-SrO/HA

Deionized water (200 mL) was mixed with 200 µL of NH_3 25% as the catalyst and stirred at 500 rpm for 15 min. Then, 6.93 g of TEOS and 10.71 g of $CaCO_3$ were added and stirred for 30 min [14]. $Al(NO_3)_3$ 0.74 g and 0.71 g $SrCO_3$ were added and stirred for 30 min. The mixture was stirred and heated at 60 °C for 12 h to obtain a dry gel, then calcined at 1000 °C for 3 h. The product was mixed with 1.3 g Bi_2O_3 to obtain a product with a composition of 20% SiO_2, CaO 60%, Al_2O_3 2%, SrO 5%, and Bi_2O_3 13%, called MTA modified with 5% SrO (MTA-SrO5). Similar works were performed by varying the weight of $SrCO_3$ and Bi_2O_3 to obtain the total percentage of SrO and Bi_2O_3 of 18%. The selected MTA-SrO (10 g) was then added with hydroxyapatite (HA) in various weights (0.3, 0.6, and 0.9 g) to acquire the percentages of 3, 6, and 9%, respectively. The multiple percentages of $SrCO_3$, Bi_2O_3, and HA in MTA and the product codes are presented in Table 1. The products were ground with a mortar and sieved through a 200-mesh sieve. The results were characterized using XRD and FTIR. The selected MTA modified with SrO and HA were identified with TGA-DTA, SEM, and XRF.

Hydration of MTA materials

The products (1.5 g) were hydrated by mixing with 0.5 g distilled water (the weight ratio of powder to water 3:1) until a homogeneous mixture was obtained. The

Table 1. Composition of modified MTA

Product codes	Bi_2O_3 (g)		$SrCO_3$		HA	
	(g)	(%)	(g)	(%)	(g)	(%)
MTA	1.80	18.00	0.00	0.00	0.00	0.00
MTA-SrO5	1.30	13.00	0.71	5.00	0.00	0.00
MTA-SrO7.5	1.05	10.50	1.05	7.50	0.00	0.00
MTA-SrO10	0.80	8.00	1.42	10.00	0.00	0.00
MTA-SrO5/HA3	1.30	13.00	0.71	5.00	0.30	3.00
MTA-SrO5/HA6	1.30	13.00	0.71	5.00	0.60	6.00
MTA-SrO5/HA9	1.30	13.00	0.71	5.00	0.90	9.00

mixture was molded in a template with different sizes depending on the measurement that would be performed.

Compressive strength test

The hydrated MTA was molded into specimens with a thickness of 6 mm and a diameter of 4 mm (ISO 9917-1). The compressive strength of the specimen was measured with a UTM tool after a hydration period of 14 days.

Measurement of pH, calcium ion release, and weight loss

The fresh hydrated MTA was molded into a tube with a diameter of 4 mm and a thickness of 3 mm. The specimen was placed in 2.5 mL of artificial saliva. After 14-day immersion, artificial saliva pH was measured with a pH Analyzer, and the calcium ion released was determined with AAS. The sample was removed from the saliva and dried at 90 °C for 24 h. Weight loss (m) presented in percent was calculated using Eq. (1).

$$m(\%) = \frac{W_i - W_f}{W_i} \times 100 \quad (1)$$

W_i and W_f are sample weights of initial (before) and final (after) immersion, respectively. This method refers to the ISO-6876 procedure for determining solubility.

Radiopacity

A freshly hydrated MTA sample was molded into a tube with a diameter and thickness of 5 and 1 mm, respectively. After 24 h, the materials were irradiated with 7 mA, 70 kV, and an X-ray source distance from a sample of 30 cm. X-ray exposures for 0.2 sec (ISO 6876). The radiopacity of commercial MTA (CMTA) was used as the comparison.

Dentin-material interaction

A freshly hydrated MTA sample was inserted into the detached human teeth and stored for 1 day. The teeth were then immersed in an artificial saliva solution for 7 days and cut horizontally. The excised teeth were observed with SEM to identify the morphology and dentin-MTA interface interaction.

■ RESULTS AND DISCUSSION

DTG/TGA

The process in the sample calcination was predicted by evaluating the weight lost during heating on the DTA/TGA measurements. The MTA sample modified with SrO 5% was selected as the representative sample. The TGA/DTA data are presented in Fig. 1.

Fig. 1 shows that the total weight loss of the MTA-SrO5 gel during heating to 1200 °C was 26.9%. The release of water molecules from the sample occurred

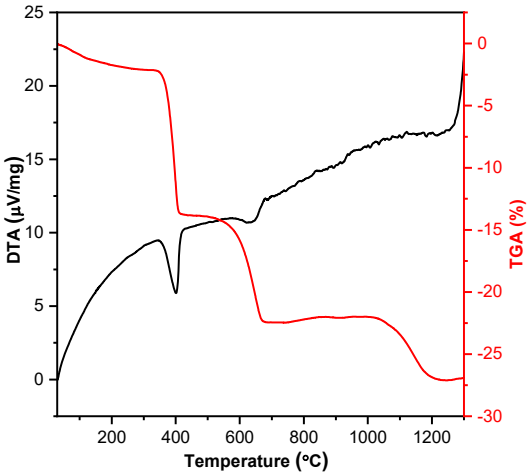

Fig 1. TGA/DTA MTA-SrO5

endothermically at 200 °C with a weight loss of 1.73%. The exothermic process at 400 °C could be attributed to gas decomposition, the release of H_2O from portlandite ($Ca(OH)_2$), and formed oxide compounds. The endothermic reaction of decomposition calcite ($CaCO_3$) to CaO and CO_2 at 625–650 °C. This reaction was accompanied by mass loss on the thermogravimetric curve (17.74%). The exothermic process of C_3S and C_2S crystal formation occurred at 1000–1100 °C. The endothermic process from carbonate molecules bound to $SrCO_3$ was broken down into SrO at 1050–1150 °C with a total mass loss of 23.44% from starting material. Ideal conditions to form calcium silicate were conducted by crushing for 8 h and followed by calcination at 1000 °C for 2 h. The heating temperature range at 800–1000 °C cannot affect the change in the calcium silicate stage [15]. Based on the thermal analysis results for the hardened material identification, the starting material was heated at 1000 °C for 3 h.

XRD Patterns of MTA Materials

XRD test result data processing was done using origin software and analyzed using match 3! software, then compared with JCPDS data. After calcination, the formed MTA components were identified with XRD. The XRD patterns are presented in Fig. 2. The diffractogram of MTA (Fig. 2(a)) showed a peak at (2θ) 18° corresponding to $Ca(OH)_2$ portlandite (ICDD 44-1481). The characteristics peak at (2θ) 28.6° was related to C_3S (ICDD 31-0301 and JCPDS 42-0551), (2θ) 32.1° was assigned to overlap C_3S and C_2S, (2θ) 33.5° was C_3S and $SrSiO_3$, and (2θ) 27, 28.4 and 46.5° were Bi_2O_3 as radiopacity agent [7]. The radiopacity agent showed physical interactions after the calcination process. The presence of tricalcium silicate (C_3S) indicates the success of MTA synthesis. The overlapping C_3S and C_2S cause an indefinite crystal-phase quantity of components in the material. As a result, the structure of the MTA material cannot be known.

Based on Fig. 2(b–d), peaks (2θ) 18° increased by increasing the SrO quantity. The peak of strontium silicate (2θ) 33.5° (JCPDS No. 36-0018) increased with the addition of SrO to the material. This finding indicates that SrO has entered the MTA material, reacted with silica to form strontium silicate by solid reaction, and substituted calcium in the crystal structure. The occurrence of substitution is also supported by a decrease in the C_3S peak at (2θ) 32.1°. The peak at (2θ) 28.6° in MTA showed a high intensity, but the peak decreased after adding 5% SrO, and the peak was higher with the addition of SrO (SrO7.5 and SrO10).

Based on Fig. 2(f–h), HA appeared at 2θ of 25.8° (002); 34° (202); and 49.9° (213) (JCPDS No. 00-009-0432). The intensity peak at 2θ of 25.8° increased with the increasing quantity of HA (3, 6, 9%). The peak was detected as calcium phosphate.

FTIR Spectra of MTA Materials

FTIR analysis was used to determine the peak of the compound from the results of molecular vibrations.

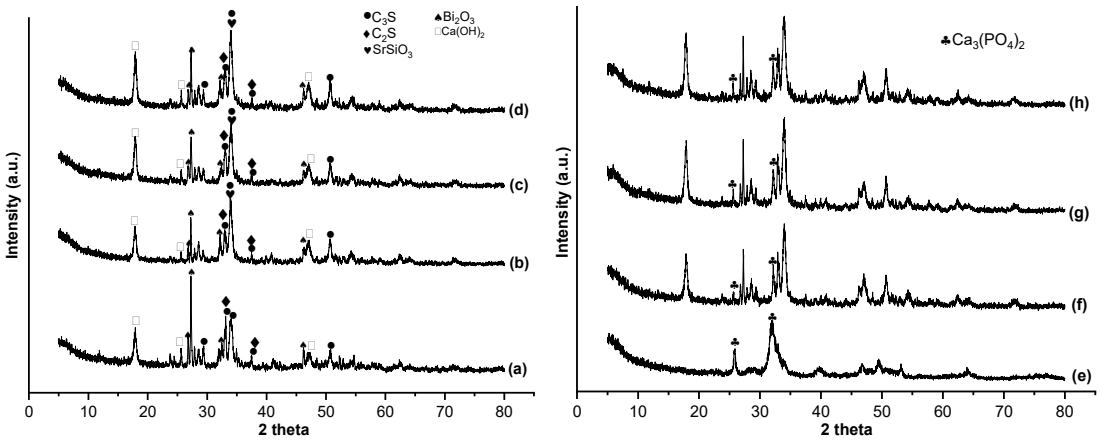

Fig 2. XRD patterns of (a) MTA, (b) MTA-SrO5, (c) MTA-SrO7.5, (d) MTA-SrO10, (e) HA, (f) MTA-SrO5/HA3, (g) MTA-SrO5/HA6, (h) MTA-SrO5/HA9

Based on the results of the FTIR test, the peak analysis can be seen in Table 2.

Based on the FTIR spectra as presented in Fig. 3(a), the characteristics of MTA powder could be seen from the peak of 879 cm^{-1} assigned to Si-O-Ca of C_3S [16-18]. The addition of SrO also decreases the intensity at 879 and 995 cm^{-1} and causes the peak shift to a smaller wavenumber, although it is insignificant. This shifting is due to the interaction of SrO and other oxides in material or substitution. This argument can be proven by further analysis to determine the occurrence of calcium substitution by strontium.

Based on Fig. 3(a-c), a vibration at 3641 cm^{-1} increased with increasing SrO to the addition of 7.5 w/w in the material and decreased after 10 w/w addition. This increment is due to the chemical interaction in the MTA component with SrO. It can be said that the optimum interaction of SrO with the MTA component was 7.5 w/w addition.

The bands at 1041 and 1458 cm^{-1} correspond to the HA stretching and bending vibrations of PO_4^{3-}, respectively [19]. The more HA added to MTA-SrO5, the greater the intensity of PO_4^{3-}. This finding is due to the phosphate ions contained in HA, which are added physically to the MTA-SrO5 material. The addition of HA to MTA-SrO5 (Fig. 3(f-h)) samples also causes a split peak at 1458 cm^{-1}. The more HA added, the steeper the split peak at 879 cm^{-1}. This splitting peak was because the HA contained calcium, so there was an increase in the amount of calcium and the addition of HA.

XRF Analysis

XRF analysis was used to determine the material components in the form of atoms or oxide compounds. XRF test results can be seen in Table 3.

Based on Table 3. after thermal treatment, the composition of MTA corresponds to the calculation of 18%. The SrO components in the MTA-SrO5 and MTA-SrO5/HA samples followed the calculation of 5%, and the calcium oxide (CaO) components experienced a

Table 2. Wavenumber and functional groups of MTA

Wavenumber (cm^{-1})	Functional groups
879	Si-O-Ca of C_3S
995	Si-O-Ca of C_2S
1473	Ca-O stretching
1635	–OH bending of H_2O (small peak)
3448	–OH stretching of H_2O (broad peak)
3641	–OH stretching of $Ca(OH)_2$ portlandite (sharp peak)

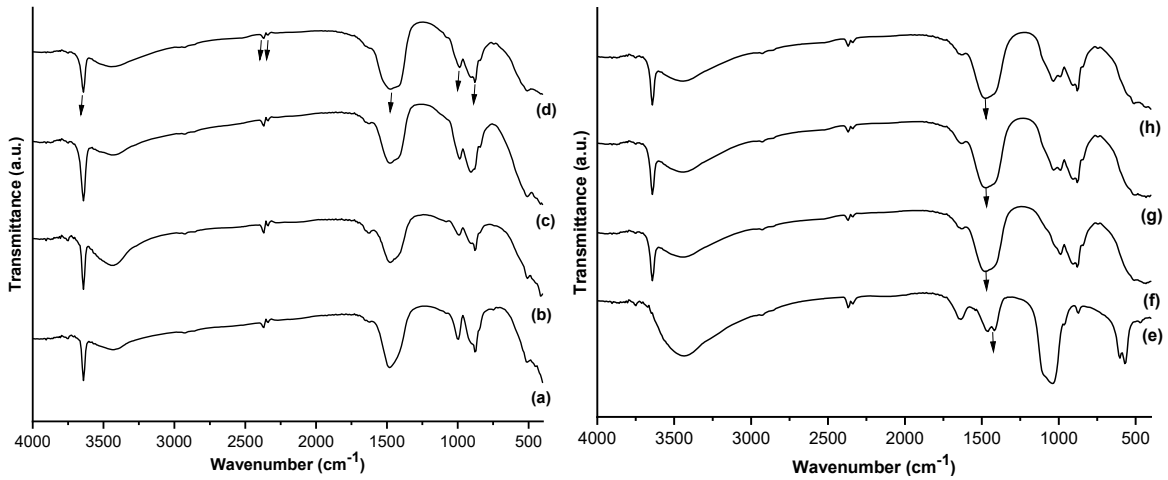

Fig 3. FTIR spectra of (a) MTA, (b) MTA-SrO5, (c) MTA-SrO7.5, (d) MTA-SrO10, (e) HA, (f) MTA-SrO5/HA3, (g) MTA-SrO5/HA6, (h) MTA-SrO5/HA9

Table 3. Composition of MTA materials

Sample	CaO	SiO_2	Bi_2O_3	SrO	P_2O_5
MTA	71.00	6.40	17.50		-
MTA-SrO5	74.00	7.55	8.30	6.00	-
MTA-SrO5/HA6	76.70	7.62	7.71	5.39	2.55

percentage increase compared to the initial calculation. The loss of water and the formation of portlandite increase the CaO levels, which then turn into CaO due to calcination. In addition, the NH_3 catalyst used can increase the percentage of $CaCO_3$, thus, increasing the CaO levels. The XRD peaks of tricalcium silicate will continue to increase as the thermal treatment temperature increases and the component or degree of the compound crystallinity increases [20].

Calcination may decrease silicon dioxide levels, which is analogous to calcium. Thereby, the CaO levels also increase. The peak intensity of silanol and siloxane will decrease with the increasing calcination temperature, validated by the FTIR test [21]. The added strontium is usually 5%, 10%, or 17.5 mol to obtain the best bioactivity [22]. The SrO level of 8% that can react with HA increases the mineralization. As a result, the level of material substitution in teeth can be more optimal [23].

Mechanical Compressive Strength

Mechanical compressive strength was measured after 14 days hydration in a specimen (d = 4 mm, h = 6 mm) [17,24]. Hydration was carried out with an MTA/water weight ratio of 3:1 [25]. The compressive strength of MTA samples after 14 days is presented in Fig. 4.

Based on Fig. 4, SrO increases the compressive strength of MTA significantly. The optimum addition of SrO to MTA was 5%. Hence, the composition was then used to study the effect of HA on the MTA-SrO properties. However, adding more than 5% SrO (SrO7.5 and SrO10) reduced the compressive strength. This reduction is probably due to the presence of SrO that does not react with other components, causing the material to become brittle. The presence of SrO may increase the surface area, microhardness, and mechanical strength and simultaneously decrease the porosity [26]. Fig. 4 shows that the sample used as medicament materials having almost the same compressive strength as the commercial MTA (CMTA) is MTA-SrO5/HA6 sample. The addition of HA substantially improves the compressive qualities by 65 and 72% for Portland cement, 280 and 197% for GMTA, and 170 and 122% for MTA, separately [27]. Adding 6% hydroxyapatite to the MTA-SrO5 increases the compressive quality over CMTA as a control (17.80 ± 1.25). The compressive strength is also affected by hybrid MTA with HA that produces alkaline pH but has no effect on the structure or mineralization of MTA and significantly increases the compressive strength of 65 and 72% for Portland cement [27].

One factor for the low mechanical strength of synthetic MTA is that bismuth oxide does not take part

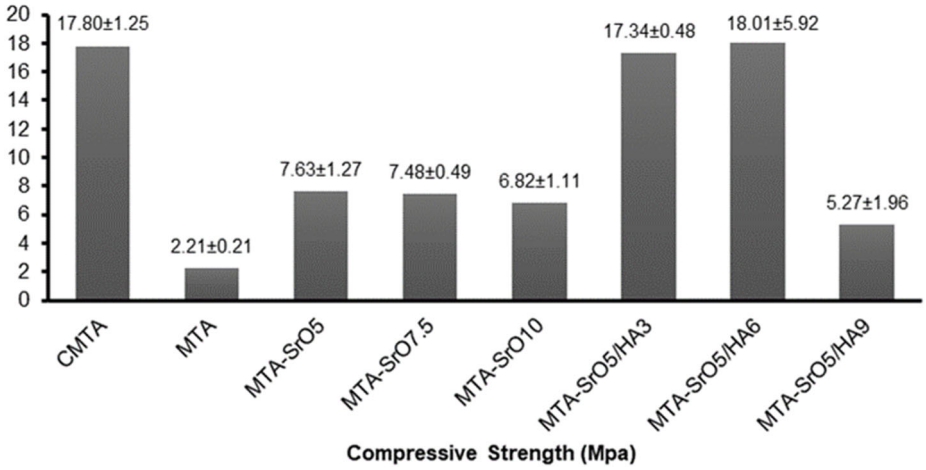

Fig 4. Compressive strength of specimens after 14 days of hydration

in the hydration of MTA reaction and can lead to defect formation in cement, thereby reducing the material's mechanical strength [28]. Adding more than 10% bismuth can increase the porosity and decrease the compressive strength value [29]. The change in porosity is because the dense structure of MTA is due to the effect of the composite form of the five oxides aggregating in the presence of water during hydration.

pH Material

Data on pH, calcium ion release, and mass reduction depend on material characteristics. The data on calcium ion release, pH, and weight loss after 14 days of immersion in artificial saliva, are presented in Table 4.

Based on the pH test results in Table 4, a base pH can facilitate cement formation, and a stable pH condition indicates that the cement has been formed successfully. All MTA samples have a stable pH for a 14-day measurement period because of the stable release of -OH. All samples had pH values larger than CMTA. These higher pH values indicate that the stable release of hydroxyl ions is affected by the hardness of the material in a humid environment. MTA-SrO5 had the highest pH value of other samples. A high pH value (alkaline pH) will create a sterile environment so that the material has high biocompatibility and antibacterial properties in MTA [30].

An indication of the biological properties of MTA is associated with alkaline pH and stable calcium ion-releasing capacity. An alkaline pH for a long time is one of the bioactivity capabilities of sealer materials [31]. The alkaline pH is also affected by the addition or hybrid of MTA with HA but does not affect the structure and mineralization of MTA [27]. In dental materials, high alkalinity can help mineralize hard tissues and provide good antimicrobial activity [32]. Alkaline pH can make the cell membrane enzymes inactive through the termination of biological activities and can inhibit some bacteria, especially *E. faecalis* [33]. Conversely, materials with a low pH will cause tooth erosion because the teeth are exposed to acid continuously [34].

Calcium Ion Release

As seen in Table 4, at 14-days of immersion, the sample with the lowest calcium release was MTA-SrO5/HA6. This indicates that the cement has been formed stably. The graph trend of CMTA increased after 14 days (15.66 ± 1.96) of immersion, and cement could be stable after 28 days of immersion [35]. Based on the synthesized MTA, a stable release of calcium ions occurred with the addition of SrO 5% and HA 6%. This value indicates that cementation has progressed well, where the release of calcium ions is the lowest compared to the others. The reduced concentration of Ca^{2+} ions released from the MTA sample over time is due to the cement hardening process [36].

The hydrated calcium silicate of the material can provide bioactivity due to the release of Ca^{2+} and OH^{-}. At alkaline pH conditions, calcium ions can dissolve and interact with phosphates in body fluids [12]. Ca^{2+} ions can combine with phosphate ions from saliva to form an apatite deposit. This combination causes bioactivity and compressive strength of the material [37]. Thus, they can function as antibacterial, and the material is as good as hydroxyapatite by forming hard tissues. SrO can control calcium ions released from the material to reduce the

Table 4. pH, calcium ion release, and weight loss after 14 days of immersion in artificial saliva

Samples	pH	Ca ion release (ppm)	Weight loss (%)
CMTA	7.91 ± 0.00	35.25 ± 0.00	2.69 ± 0.00
MTA	8.09 ± 0.01	68.91 ± 8.36	3.03 ± 0.40
MTA-SrO5	8.33 ± 0.04	23.15 ± 1.00	4.18 ± 0.81
MTA-SrO7.5	8.04 ± 0.02	29.60 ± 1.46	2.46 ± 1.53
MTA-SrO10	8.13 ± 0.03	25.06 ± 1.47	0.59 ± 0.48
MTA-SrO5/HA3	8.05 ± 0.08	22.83 ± 3.03	1.58 ± 0.25
MTA-SrO5/HA6	8.08 ± 0.05	16.95 ± 3.06	1.26 ± 0.73
MTA-SrO5/HA9	8.02 ± 0.12	18.75 ± 6.33	0.86 ± 0.70

the concentration of calcium ions released. SrO also significantly initiates calcium ions' release, thereby increasing hard tissue regeneration [26].

Weight Loss

The release of Ca ions will also affect weight loss. In addition to calcium ions, the MTA materials that have less aggregation with the hydrated materials will also be released after immersion. This release will affect the weight loss of the MTA material after hydration. Based on Table 4, mass reduction after 14 days is less than CMTA and MTA, indicating that cement formation is stable so that the material becomes sticky, and no material is lost from the cement. On day 14, there was a stable and less mass reduction for the material added with SrO and HA (MTA-SrO5/HA6). The lowest weight loss properties were found in the MTA-SrO10 sample after 14 days. This weight loss indicates that MTA is stable and not easily dissolved by the presence of liquid in the tissue. The low weight loss of the material can prevent the leakage of microorganisms into the dental tissue [4].

Artificial saliva is used for immersion because its characteristics are similar to biological systems in humans compared to deionized water [38]. In artificial saliva, there are phosphate ions that allow the formation of hydroxyapatite $Ca_5(PO_4)_3(OH)$ deposits. The apatite precipitate is obtained from the dissolution of calcium hydroxide formed after immersion, affecting the weight loss of MTA [37].

Weight loss is related to the number of calcium ions released and the pH of the solution. The more weight loss material, the higher the calcium ions and hydroxyl groups released in the solution. Therefore the pH becomes alkaline. Based on this explanation, the samples from the synthesized MTA and CMTA were better in pH values, the release of calcium ions, compressive strength, and weight loss, and could form more stable cement for 14 days of cementation MTA-SrO5/HA6.

Radiopacity

The results of the radiopacity characterization can be seen in Fig. 5. The results of the radiopacity test with an aluminum wedge thickness standard can be seen in Table 5.

The radiopacity of MTA is affected by the presence of Bi_2O_3 and SrO. The minimum radiopacity level used as a medicament material was 3 mm Al. Based on the radiopacity test, all MTA samples are qualified as medicament materials with a thickness of more than 3 mm Al. The radiopacity values of MTA were above the standard recommended by ISO No. 6876 and ANSI/ADA No. 57 (3 mm Al). In contrast, the CMTA had a thickness of 6.46 ± 0.39 mm Al. In addition, CMTA had a radiopacity of 6.4–8.5 mm Al as a sealer and restorative material for clinical applications [39].

One of the physical properties that MTA must have as filler in a root canal is to have radiopacity properties that meet ISO standards so that it can be visualized and studied in its interaction with tooth root canals. Dental materials need to be added with radiopacifier materials,

Table 5. Test results of MTA-SrO radiopacity

Samples	Radiopacity thickness (mm Al)
MTA	5.05 ± 1.09
MTA-SrO5	5.73 ± 0.65
MTA-SrO7.5	3.14 ± 0.30
MTA-SrO10	3.97 ± 1.54
MTA-SrO5/HA3	4.41 ± 0.77
MTA-SrO5/HA6	4.21 ± 1.64
MTA-SrO5/HA9	3.51 ± 0.03

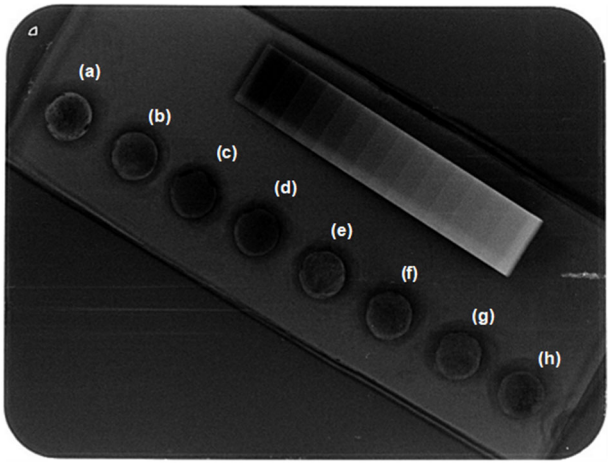

Fig 5. Results of radiopacity characterization of (a) CMTA, (b) MTA, (c) MTA-SrO5, (d) MTA-SrO7.5, (e) MTA-SrO10, (f) MTA-SrO5/HA3, (g) MTA-SrO5/HA6, and (h) MTA-SrO5/HA9

such as Bi_2O_3 and SrO. Bi_2O_3 is a metal oxide powder that is non-reactive and capable of imparting radiopaque properties to MTA [40]. Bismuth oxide is added after the thermal treatment process because the melting point of bismuth oxide is low at around 815 °C. The amount of Bi_2O_3 added to the material as a radiopacifier agent was 17–18% [4].

Dentin-material Interaction

The dentin-material interaction characteristics were used to determine the adhesion between the MTA material and the dentin layer of the teeth. MTA materials can form a dentinal bridge and become hard tissue with the dentin over time. The results of the dentin-material interaction test can be seen in Fig. 6.

The gap or microleakage between the dentin and CMTA materials was < 9 μm with a particle size of < 10 μm using the SEM test [41]. Based on Fig. 6, CMTA had a gap of about 8.85–9.37 μm. The synthesized MTA had a gap of about 2.41 μm, and MTA-SrO5 had a microleakage of less than 1 μm. MTA-SrO5 samples had smaller gab than CMTA as control and synthesized MTA. There were almost no gaps in the MTA-SrO5/HA6 samples, and it wasn't easy to distinguish between the dentin and the material. The MTA-SrO5/HA6 sample also had small gaps at certain sides.

These results show that adding SrO particles can increase the adhesion between the material and the tooth's dentin layer and decrease the gap. The SrO particles can reduce the gaps with an even distribution of each material in the MTA. SrO also initiates the calcium ions released significantly, thereby increasing hard tissue mineralization through cell proliferation [26]. The modification of MTA using SrO can increase the potential for hard-tissue formation due to the high release of calcium ions.

Meanwhile, adding HA can significantly increase the adhesion of the material with dentin and minimize gab. HA had a small calcium phosphate component and filled the gaps in the MTA material. The presence of calcium and phosphate ions in the material causes the formation of a hydroxyapatite layer at the interface. Finally, a biological bond occurs between the material and dentin, which also has the main structure of hydroxyapatite [42]. The presence of SrO and HA particles can increase the adhesion between the dentin

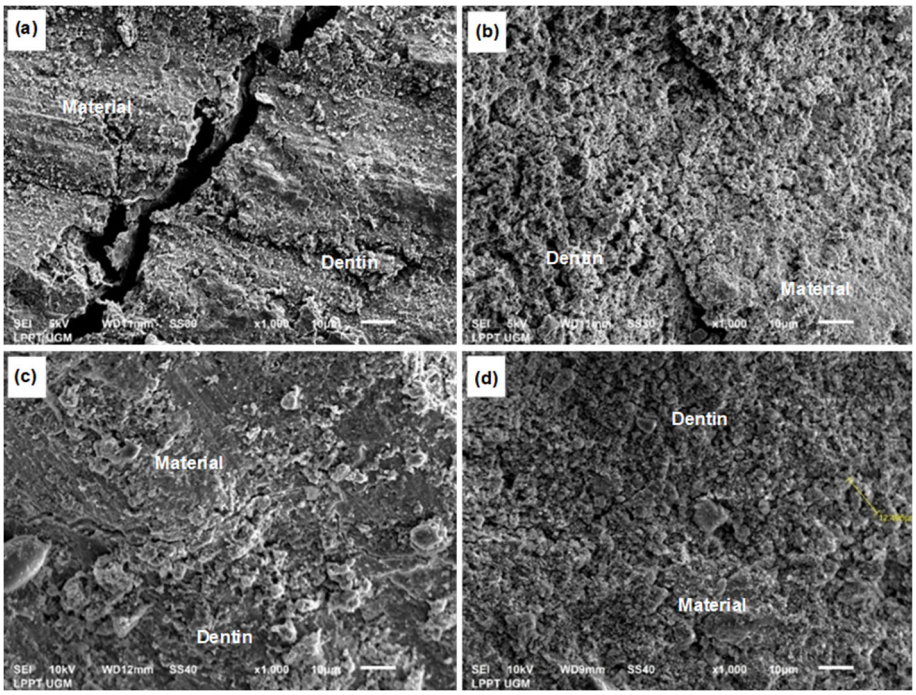

Fig 6. SEM images representing the interaction between dentin surface and (a) CMTA, (b) MTA, (c). MTA-SrO5, and (d) MTA-SrO5/HA6

layer and material, thereby increasing the compressive strength of the MTA material. The synthesized MTA-SrO5/HA6 can potentially be applied to hard tissues such as dental pulp.

■ CONCLUSION

The SrO and HA-modified MTA have been successfully synthesized and characterized. Modified MTA with SrO 5% and HA 6% showed the optimum composition, providing the highest compressive strength and potent interaction with the dental surface. The compressive strength was higher than the control, and MTA-SrO0 (17.80 ± 1.25 and 2.21 ± 0.21 MPa) became 18.01 ± 5.92 MPa after 14 days of hydration. Gabs between dentin and material also changed to be more adhesive than control. MTA-SrO0, MTA-SrO5 (8.85, 2.41, and < 1 μm) became no gabs. Moreover, adding SrO and HA to MTA increased the pH material, decreased weight loss, and released Ca^{2+} ions. Therefore, MTA-SrO5/HA6 is a potential material to be implemented as a dental material. However, further investigations on biocompatibility and in vivo tests still need to be conducted.

■ ACKNOWLEDGMENTS

This work was funded by research allowance from the LPDP RI 2022 with Fund Request number FR312022277382.

■ REFERENCES

[1] Flores-Ladesma, A., Santana, F.B., Bucio, L., Arenas-Alatorre, J., Faraji, M., and Wintergerst, A., 2017, Bioactive materials improve some physical properties of an MTA-like cement, *Mater. Sci. Eng., C*, 71, 150–155.

[2] Tawil, P.Z., Duggan, D.J., and Galicia, J.C., 2015, Mineral trioxide aggregate (MTA): Its history, composition, and clinical applications, *Compend. Contin. Educ. Dent.*, 36 (4), 247–264.

[3] Macwan, C., and Deshpande, A., 2014, Mineral trioxide aggregate (MTA) in dentistry: A review of literature, *J. Oral Res. Rev.*, 6 (2), 71–74.

[4] Prasad, K., and Naik, C.T., 2017, Mineral trioxide aggregate in endodontics, *Int. J. Appl. Dent. Sci.*, 3 (1), 71–75.

[5] Nishad, K.V., Manoj, K., and Unnikrishnan, G., 2019, Synthesis of strontium orthosilicate (Sr_2SiO_4) by sol-gel method, for the use in endodontic cements to enhance bioactivity and radio-contrast, *Mater. Res. Express*, 6, 105401.

[6] Bakhit, A., Kawashima, N., Hashimoto, K., Noda, S., Nara, K., Kuramoto, M., Tazawa, K., and Okiji, T., 2018, Strontium ranelate promotes odonto-/osteogenic differentiation/mineralization of dental papillae cells *in vitro* and mineralized tissue formation of the dental pulp *in vivo*, *Sci. Rep.*, 8 (1), 9224.

[7] Abd El-Hamid, H.K., Abo-Almaged, H., dan Radwan, M., 2017, Synthesis, characterization, and antimicrobial activity of nano-crystalline tricalcium silicate bio-cement, *J. Appl. Pharm. Sci.*, 7 (10), 1–8.

[8] Ressler, A., Cvetnić, M., Antunović, M., Marijanović, I., Ivanković, M., and Ivanković, H., 2020, Strontium substituted biomimetic calcium phosphate system derived from cuttlefish bone, *J. Biomed. Mater. Res., Part B*, 108 (4), 1697–1709.

[9] Swarup, S.J., Rao, A., Boaz, K., Srikant, N., and Shenoy, R., 2014, Pulpal response to nano hydroxyapatite, mineral trioxide aggregate and calcium hydroxide when used as a direct pulp capping agent: An in vivo study, *J. Clin. Pediatr. Dent.*, 38 (3), 201–206.

[10] Hanafy, A.K., Shinaishin, S.F., Eldeen, G.N., and Aly, R.M., 2018, Nano hydroxyapatite & mineral trioxide aggregate efficiently promote odontogenic differentiation of dental pulp stem cells, *Open Access Maced. J. Med. Sci.*, 6 (9), 1727–1731.

[11] Kakani, A.K., Veeramachaneni, C., Majeti, C., Tummala, M., and Khiyani, L., 2015, A review on perforation repair materials, *J. Clin. Diagn. Res.*, 9 (9), ZE09–ZE13.

[12] Hosseinzade, M., Soflou, R.K., Valian, A., and Nojehdehian, H., 2016, Physicochemical properties of MTA, CEM, hydroxyapatite and nano

hydroxyapatite-chitosan dental cements, *Biomed. Res.*, 27 (2), 442–448.

[13] Agrawal, K., Singh, G., Puri, D., and Prakash, S., 2011, Synthesis and characterization of hydroxyapatite powder by sol-gel method for biomedical application, *J. Miner. Mater. Charact. Eng.*, 10 (8), 727–734.

[14] Fa'izzah, M., Widjijono, W., Kamiya, Y., and Nuryono, N., 2020, Synthesis and characterization of white mineral trioxide aggregate using precipitated calcium carbonate extracted from limestone, *Key Eng. Mater.*, 840, 330–335.

[15] Phuttawong, R., Chantaramee, N., Pookmanee, P., and Puntharod, R., 2015, Synthesis and characterization of calcium silicate from rice husk ash and shell of snail *Pomacea canaliculata* by solid-state reaction, *Adv. Mater. Res.*, 1103, 1–7.

[16] Chen, S., Shi, L., Luo, J., and Engqvist, H., 2018, Novel fast-setting mineral trioxide aggregate: Its formulation, chemical-physical properties, and cytocompability, *ACS Appl. Mater. Interfaces*, 10 (24), 20334–20341.

[17] Li, Q., and Coleman, N.J., 2015, The hydration chemistry of ProRoot MTA, *Dent. Mater. J.*, 34 (4), 458–465.

[18] Lee, B.S., Lin, H.P., Chan, J.C.C., Wang, W.C., Hung, P.H., Tsai, Y.H., and Lee, Y., 2018, A novel sol-gel-derived calcium silicate cement with short setting time for application in endodontic repair of perforations, *Int. J. Nanomed.*, 13, 261–271.

[19] Khoiruddin, M., Yelmida, Y., and Zultiniar, Z., 2015, Sintesis dan karakterisasi hidroksiapatit (Hap) dari kulit kerang darah (*Anadara granosa*) dengan proses hidrotermal, *JOM FTEKNIK*, 2 (2), 1–8.

[20] Voicu, G., Bădănoiu, A., Ghiţulică, C., and Andronescu, E, 2012, Sol-gel of white mineral tioxide aggregate with potential use as biocement, *Dig. J. Nanomater. Biostruct.*, 7 (4), 1639–1646.

[21] Ummah, S., Prasetyo, A., and Barroroh, H., 2010, Kajian penambahan abu sekam padi dari berbagai suhu pengabuan terhadap plastisitas kaolin, *Alchemy*, 1 (2), 70–74.

[22] Zhu, H., Guo, D., Sun, L., Li, H., Hanaor, D.A.H., Schmidt, F., and Xu, K., 2018, Nanostructural insights into the dissolution behavior of Sr-doped hydroxyapatite, *J. Eur. Ceram. Soc.*, 38 (16), 5554-5562.

[23] Ehret, C., Aid-Launais, R., Sagardoy, T., Siadous, R., Bareille, R., Rey, S., Pechev, S., Etienne, L., Kalisky, J., de Mones, E., Letourneur, D., and Vilamitjana, J., 2017, Strotium-doped hydroxyapatite polysaccharide materials effect on ectopic bone formation, *PLoS One*, 12 (9), e0184663.

[24] Kim, M., Yang, W., Kim, H., and Ko, H., 2014, Comparison of biological properties of ProRoot MTA, OrthoMTA, and Endocem MTA cements, *J. Endod.*, 40 (10), 1649–1653.

[25] Basturk, F., Nekoofar, M.H., Gunday, M., and Dummer, P.M.H., 2015, Effect of varying water-to-powder ratios and ultrasonic placement on the compressive strength of mineral trioxide aggregate, *J. Endod.*, 41 (4), 531–534.

[26] Saghiri, M.A., Asgar, K., Lotfi, M., and Garcia-Godoy, F., 2012, Nanomodification of mineral trioxide aggregate for enhanced physiochemical properties, *Int. Endod. J.*, 45 (11), 979–988.

[27] Alqedairi, A., Muñoz-Viveros, C.A., Pantena, E.A., Campillo-Funollet, M., Alfawas, H., Abou Neel, E.A., and Abuhaimed, T.S., 2017, Superfast set, strong, and less degradable mineral trioxide aggregate cement, *Int. J. Dent.*, 2017, 3019136.

[28] Tanomaru-Filho, M., Morales, V., da Silva, G.F., Bosso, R., Reis, J.M.S.N., Duarte, M.A.H., and Guerreiro-Tanomaru, J.M., 2012, Compressive strength and setting time of MTA and Portland cement associated with different radiopacifying agents, *ISRN Dent.*, 2012, 898051.

[29] Coomaraswamy, K.S., Lumley, P.J., and Hofmann, M.P., 2007, Effect of bismuth oxide radioopacifier content on the material properties of an endodontic Portland cement-based (MTA-Like) system, *J. Endod.*, 33 (3), 295–298.

[30] Malhotra, N., Agarwal, A., and Mala, K., 2013, Mineral trioxide aggregate: A review of physical

properties, *Compend. Contin. Educ. Dent.*, 34 (2), e25–e32.

[31] Bortoluzzi, E.A., Broon, N.J., Bramante, C.M., Garcia, R.B., de Moraes, I.G., and Bernardineli, N., 2006, Sealing ability of MTA and radiopaque Portland cement with or without calcium chloride for root-end filling, *J. Endod.*, 32 (9), 897–900.

[32] Shekhar, S., Jaiswal, S., Nikhil, V., Gupta, S., Mishra, P., and Raj, S., 2019, Comparative pH and calcium ion release in newer calcium silicate-based root canal sealers, *Endodontology*, 31 (1), 29–33.

[33] Ghazvini, S.A., Tabrizi, M.A., Kobarfard, F., Baghban, A.A., and Asgary, S., 2009, Ion release and pH of a new endodontic cement, MTA and Portland cement, *Iran. Endod. J.*, 4 (2), 74–8.

[34] Mark, A.M., 2018, What is dental erosion?, *J. Am. Dent. Assoc.*, 149 (6), 564.

[35] Gandolfi, M.G., Iezzi, G., Piattelli, A., Prati, C., and Scarano, A., 2017, Osteoinductive potential and bone-bonding ability of ProRoot MTA, MTA Plus and Biodentine in rabbit intramedullary model: Microchemical characterization and histological analysis, *Dent. Mater.*, 33 (5), e221–e238.

[36] Sawhney, S., and Vivekananda Pai, A.R., 2015, Comparative evaluation of the calcium release from mineral trioxide aggregate and its mixture with glass ionomer cement in different proportions and time, *Saudi Dent. J.*, 27 (4), 215–219.

[37] Yamamoto, S., Han, L., Noiri, Y., and Okiji, T., 2017, Evaluation of the Ca ion release, pH and surface apatite formation of a prototype tricalcium silicate cement, *Int. Endod. J.*, 50 (S2), e73–e82.

[38] Patil, S., Hoshing, U., and Rachalwar, D., 2017, Solubility of 5 different root canal sealers in water and artificial saliva, *Int. J. Curr. Res.*, 9, 61490–61493.

[39] Ha, W.N., Nicholson, T., Kahler, B., and Walsh, L., 2017, Mineral trioxide aggregate-A review of properties and testing methodologies, *Materials*, 10 (11) 1261.

[40] Li, Q., and Coleman, N.J., 2019, Impact of Bi_2O_3 and ZrO_2 radiopacifiers on the early hydration and C-S–H gel structure of white Portland cement, *Dent. Mater. J.*, 10 (4), 46.

[41] Dewi, F., Asrianti, D., and Margono, A., 2017, Microleakage evaluation of modified mineral trioxide aggregate effect toward marginal adaptation on cervical dentin perforation, *Int. J. Appl. Pharm.*, 9 (2), 10–13.

[42] Sarkar, N.K., Caicedo, R., Ritwik, P., Moiseyeva, R., and Kawashima, I., 2005, Physicochemical basis of the biologic properties of MTA, *J. Endod.*, 31 (2), 97–100.